Laser boresighting by second harmonic generation

Mike Adel, Bob Buckwald, Dario Cabib

CI Systems (Israel) Ltd.
Industrial Park, Migdal Haemek 10551, Israel

ABSTRACT

Weapons delivery systems frequently use laser designators which require boresighting with the visual line of sight. For systems based on the Nd.YAG laser ($\lambda = 1.06\mu$m), this may be achieved by a boresight collimator with a second harmonic generating crystal in its focal plane which reradiates collimated, visible light ($\lambda = 0.53\mu$m). The conception, design and testing of such a device will be described along with a comparison with alternative technologies which demonstrates its superiority in terms of conversion efficiency, damage threshold and design versatility.

1. INTRODUCTION

Laser boresighting is the process of aligning the direction of propagation of a laser designator with the line of sight of any of a number of other viewing systems such as a video camera or a Forward Looking Infra Red system[1]. In the case of a CCD or any other silicon based video camera, a Nd.YAG laser (λ=1.06μm) may be boresighted by reflection from the focal plane of a collimator into the field of view of the viewing device; see Figure 1. In many applications however, attenuators and filters in the optical system eliminate any 1.06μm wavelength light incident on the CCD, so that some form of up conversion is required from 1.06μm to visible light.

A device placed in the focal plane of the boresight collimator which upconverts pulsed 1.06μm radiation, reradiating in the 0.4 - 0.65μm wavelength range has been termed a "visual target" (VT).
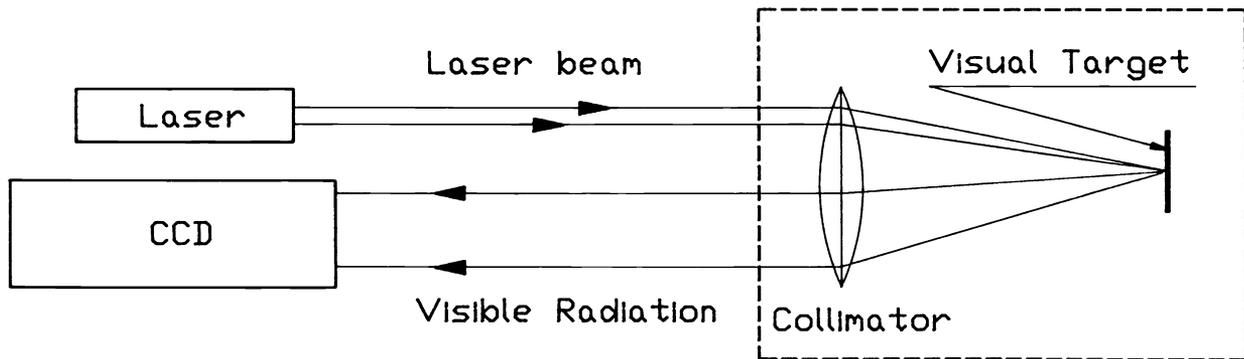
Figure 1. Schematic diagram of boresighting using the visual target method.

2. ALTERNATIVE TECHNOLOGIES

In the early developmental stages of the VT, 3 alternative technologies were considered.

2.1 Visible blackbody emission due to laser heating

A refractory ceramic or other suitable high temperature thermally stable material is placed in the focal plane of the collimator. The laser pulse causes intense local heating, resulting in temperatures of the order of 1500K which produce sufficient blackbody radiation to be observed as a bright spot in the CCD. The reemission is lambertian in geometry and increases extremely rapidly with the laser pulse energy.

2.2. Laser induced fluorescence materials

An infrared phosphor material upconverts $1.06\mu m$ radiation by two-photon absorption followed by fluorescent emission in the visible. Reemission is generally lambertian in geometry. The intensity of visible emission increases with the square of the pulse energy due to the nonlinear nature of the absorption process. The reemission intensity also reaches saturation at a certain pulse energy level as expected from a fluorescence phenomenon.

2.3. Second Harmonic Generating (SHG) crystals

This phenomenon will be described in more detail since it was the chosen technique. Classically, frequency doubling may be attributed to the non-zero value of the second order dielectric susceptibility tensor, χ'. This results in a finite response by the crystal which is proportional to the product of two independent interacting radiation fields and whose frequency is the sum of the frequencies of the two fields. χ' is non vanishing only in crystals with non centro-symmetric systems such as the sphalerite structure. For the special case in which the two interacting frequencies are equal, the up conversion efficiency is strongly enhanced by choosing a direction of propagation of incident radiation for which the refractive index for the fundamental field frequency n_ω is equal to that for the harmonic frequency $n_{2\omega}$,i.e.

$$n_\omega = n_{2\omega}. \tag{1}$$

This condition is known as phase matching[2].

The nonlinear nature of the process results again in a quadratic dependence of the harmonic output pulse energy $(E_{2\omega})$ on the fundamental pulse energy, (E_ω) i.e.

$$E_{2\omega} = k \ \frac{E_\omega^2}{\Delta tA} \tag{2}$$

Here, Δt is the laser pulse duration, A is the area of the laser spot on the crystal and k is a parameter dependent on crystal identity and optical path length in the crystal.

By introducing such a crystal in the focal plane of the collimator, collinear harmonic radiation is produced and reradiated along the optical path, as shown in Figure 2. This is a significant advantage over the first two target types in which reemission is lambertian.
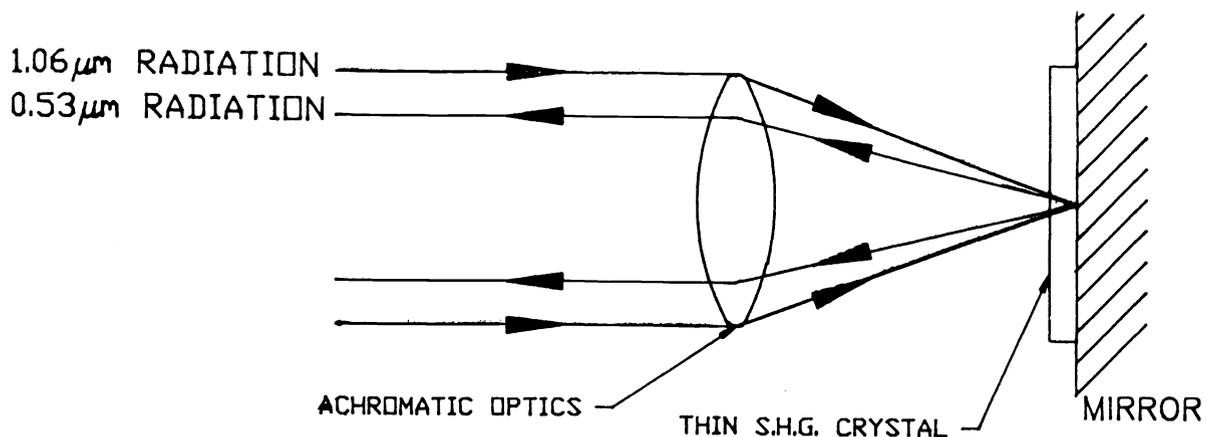
Figure 2. Schematic diagram of the application of second harmonic
generation in the visual target.

3. BASIC DESIGN CONSIDERATIONS

3.1. Target Comparison

A number of other criteria were also considered before the SHG
solution was chosen. These criteria and the results for each case
are summarized in Table 1. The results are in part due to
experiments carried out by the authors and in part theoretical
estimates, based on the literature.

It is clear from the pulse energy requirement data in the table
that the ceramic targets are much less efficient as energy
converters than either of the other two solutions. This means that
excess heat is dumped into the boresight target module which may
have effects on the function of other devices in the focal plane.
Furthermore, the energy requirement is dangerously close to the
target damage threshold experimentally determined using the same
collimator/laser specifications. In choosing between the latter
two options, the safety margin in damage threshold in addition to
the added collection efficiency due to the collimated reradiation
gave the SHG a commanding edge as the most viable solution.

Physical mechanism	Blackbody emission	Laser induced fluorescence	Second Harmonic Generation
Target type	Ceramic	Sunstone[3]	KTP (Potassium Titanyl Phosphate)
Typical required pulse energies for particular collimator /laser specifications	10^{-3}J	10^{-7}J	10^{-7}J
Single pulse damage threshold for the same collimator/ laser specifications	$10^{-3} - 10^{-2}$J	10^{-5}J	$10^{-4} - 10^{-3}$J
Reemission geometry	Lambertian, thermal spreading	Lambertian	Collimated, beam walk-off

Table 1. Comparison of different design parameters for 3 different visual target types

3.2. Crystal selection

During the research stage of the project a number of different SHG crystals were given consideration. The most important parameters for three different contenders are given in Table 2.

Since the refractive indices of the crystals are dependent on both angle of incidence and temperature, the second and third entries are given in units of [C-cm] and [mrad-cm] i.e. the length of crystal for which the fundamental and harmonic radiation remain phase matched for a given range of temperature or incidence angle respectively. Since the incident radiation is not collimated but convergent, it is important that the angular acceptance be as large as possible, in order to ensure efficient conversion. Furthermore, temperature sensitivity must be small so that target temperature fluctuations do not result in output intensity fluctuations.

Crystal Selection	(D) K.D.P.	B.B.O.	K.T.P.
Conversion efficiency @ $1MW/cm^2$ 1 cm long	0.4% +	3% +	4% +
Angular acceptance [mrad-cm]	2.2 ++	1.4 ++	13 *
Temperature bandwidth [C-cm]	6.7 ++	55 ++	20 *
Damage threshold [GW/cm^2, 1ns]	6 ++	13 ++	15 **
Crystal sensitivity	hygroscopic	-	-
Walk-off angle [mrad]	23 ++	48 ++	1-4.5 **

```
+    -    from ref [4]
++   -    from ref [5]
*    -    from ref [6]
**   -    from ref [7]
```

Table 2. Key design parameters for 3 different SHG crystals

The walk-off angle θ_w is the angle between the direction of propagation of the fundamental and harmonic wavefronts. In order to avoid boresight error, this must be small; quantitatively, it may be shown that the worst case error θ_e is given by

$$\theta_e = \frac{\ell}{f}\theta_w \tag{3}$$

where ℓ is the crystal length and f is the collimator focal length. For a KTP crystal and using for ℓ and f typical values, then $1 < \theta_e < 5\mu rad$, an acceptably small boresight error. Considering all the above factors in addition to its large damage threshold, KTP was chosen as the most suitable crystal.

3.3 Experimental

In order to demonstrate that this effect could in fact be applied in the visual target, to obtain quantitative data and to test the prototype, the experimental arrangement in Figure 3 was set up at CI. A number of different collimator configurations were used in the development of the prototype. Initially, a 2 mm long KTP crystal was placed in the focal plane of an f = 25 mm lens.
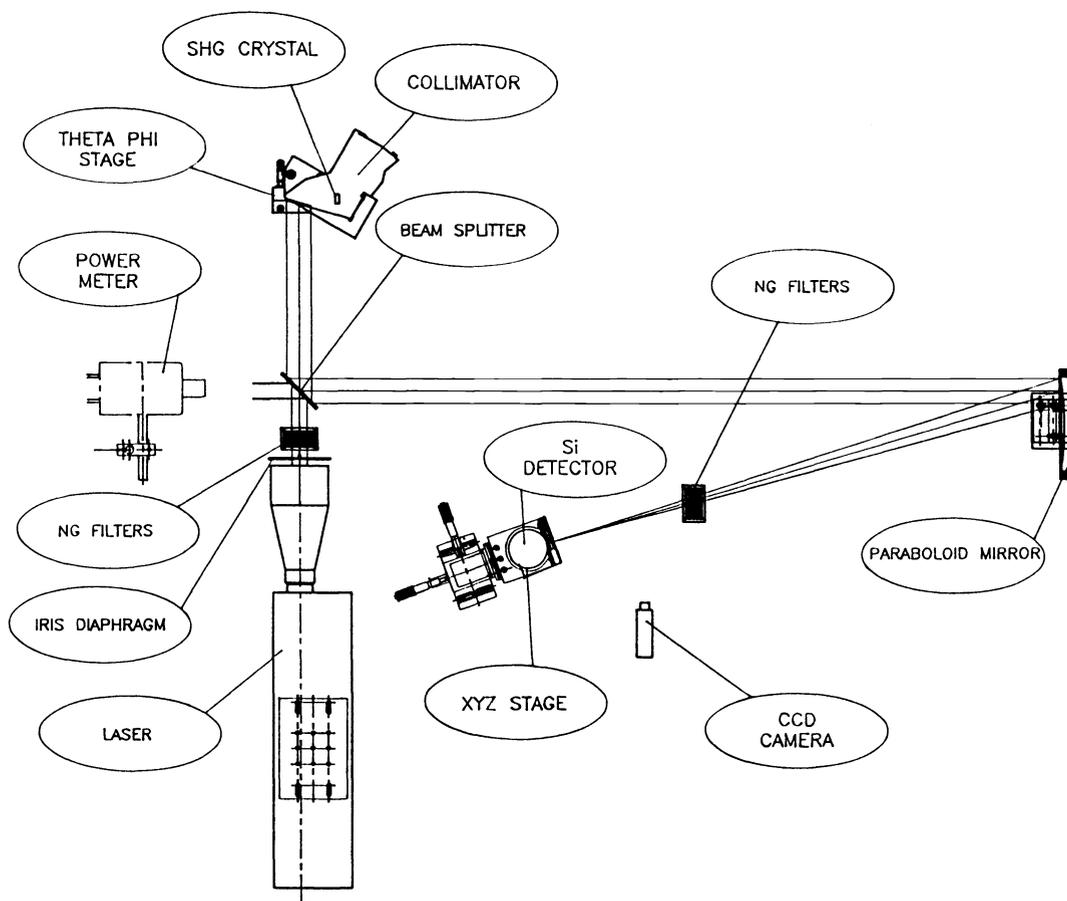
Figure 3. Experimental arrangement for investigation of the visual target.

Figure 4 shows the results obtained by varying the incident energy and measuring the energy per pulse of green radiation in a calibrated Si detector.

In fact the output pulse energy has been plotted vs the square of the input pulse energy and the linearity of the result demonstrates the quadratic dependence of equation 2. The actual conversion efficiency obtained at $0.1\mu J$ was 0.04% and increases linearly with input pulse energy.

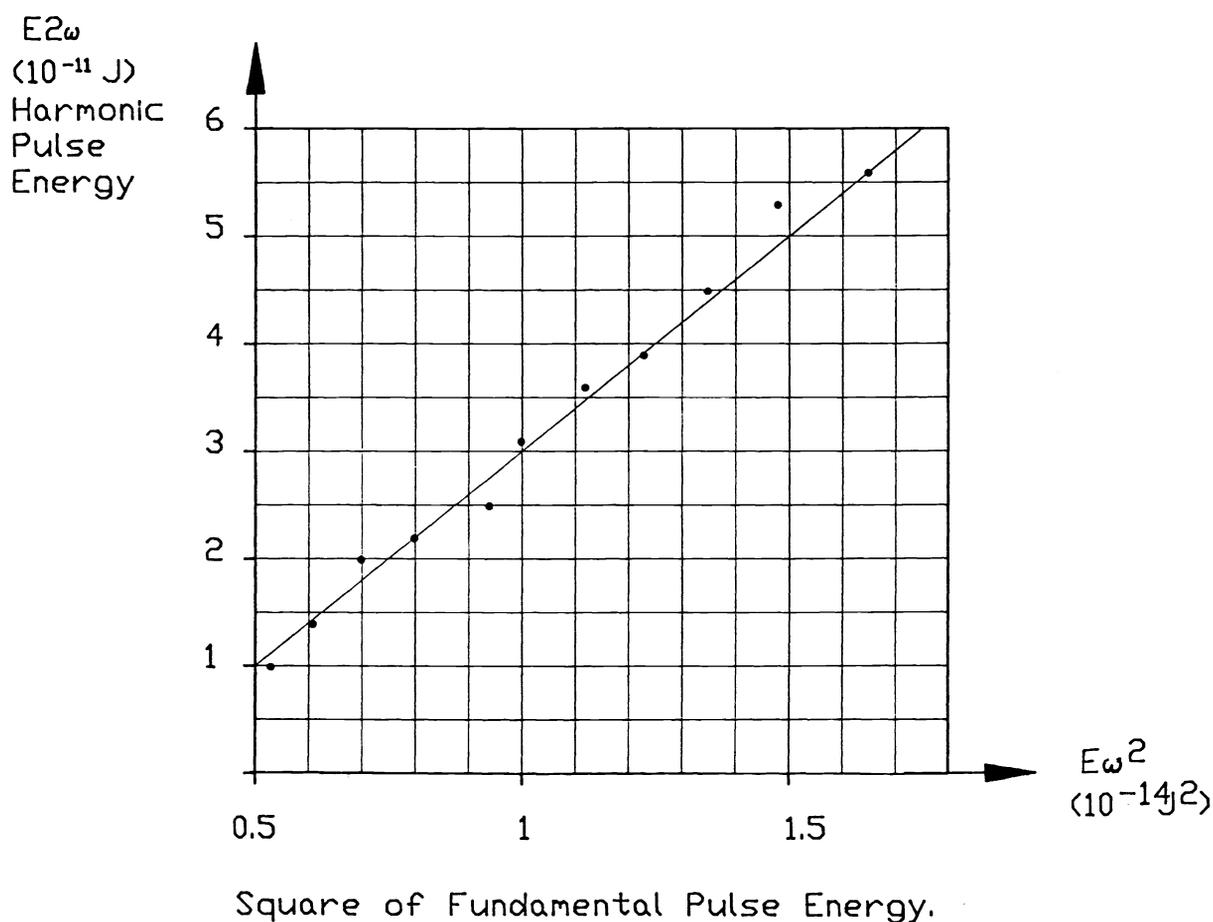
Square of Fundamental Pulse Energy.

Figure 4. Harmonic output pulse energy from a KTP crystal versus the square of the incident fundamental pulse energy for a 2 mm crystal.

The conversion efficiency dependence on angle of incidence relative to crystal normal was also measured and is shown in Figure 5.

The theoretical acceptance angle for the 2 mm long crystal used in the experiments is 3.7°. The full width half maximum of Figure 5 is approximately 9° which is significantly greater than the theoretical value, probably due to the 3.8° cone in the angle of incidence resulting from the f# of 20 for the optics in the experimental set up.

The performance dependence on temperature was also determined. The crystal was heated to 70°C using a blower and allowed to stabilize for one hour. The Si detector showed a signal intensity 70% of the value at room temperature.

The effect was also qualitatively demonstrated by focussing the green emission from the KTP crystal on the focal plane of a CCD. The visible output pulse energy $E_{2\omega}$ from the VT must lie within limits which give a good signal to noise ratio without saturating the CCD or other video device. In principle, this is achieved by varying k the conversion factor, which depends on crystal length along optical axis and beam optics for a given crystal. The other important parameters, i.e. input pulse energy, pulse duration and spot size are constrained by other system specifications. Figure 6 shows the visible pulse energy output as a function of crystal length for typical optical and beam parameters for the cases of Gaussian and Flat far field beam profiles. In the case of an non-depleted Gaussian beam whose beam waist variation is small throughout the crystal, the output power is quadratic with length[2], while for a flat profile the dependence is roughly linear with length*.

Given the specific design parameters for the system in question, calculations show that the required crystal length to obtain an acceptable pulse energy level is too small to achieve in practice. This problem is readily solved by anti-reflection coating the rear surface of the crystal to reduce the intensity of both 1.06 and 0.53 micron radiation to an acceptable level. This eliminates another predicted problem of ghost images resulting from multiple reflections within the crystal. It does however, reduce the damage threshold of the crystals.

---

*
In the case of a spot of radius r, large enough to neglect diffraction effects, it can be shown that for a flat far field beam profile convergent on an SHG crystal, the output power varies as

$$\log\left[1 + \frac{\theta\ell}{r}\right] - \frac{\theta\ell}{r + \theta\ell}$$

where θ is the half cone angle of the convergent radiation and ℓ is the crystal length.
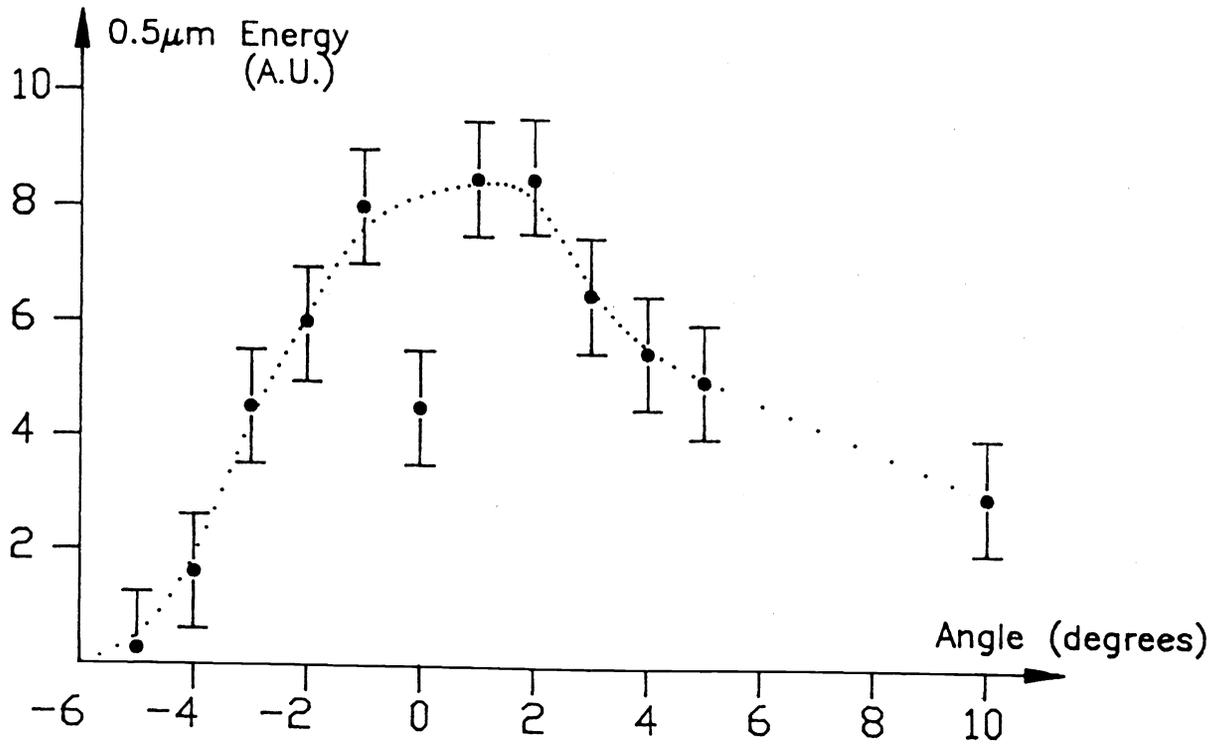
Figure 5. Harmonic output pulse energy vs angle of incidence of fundamental beam relative to crystal face normal.
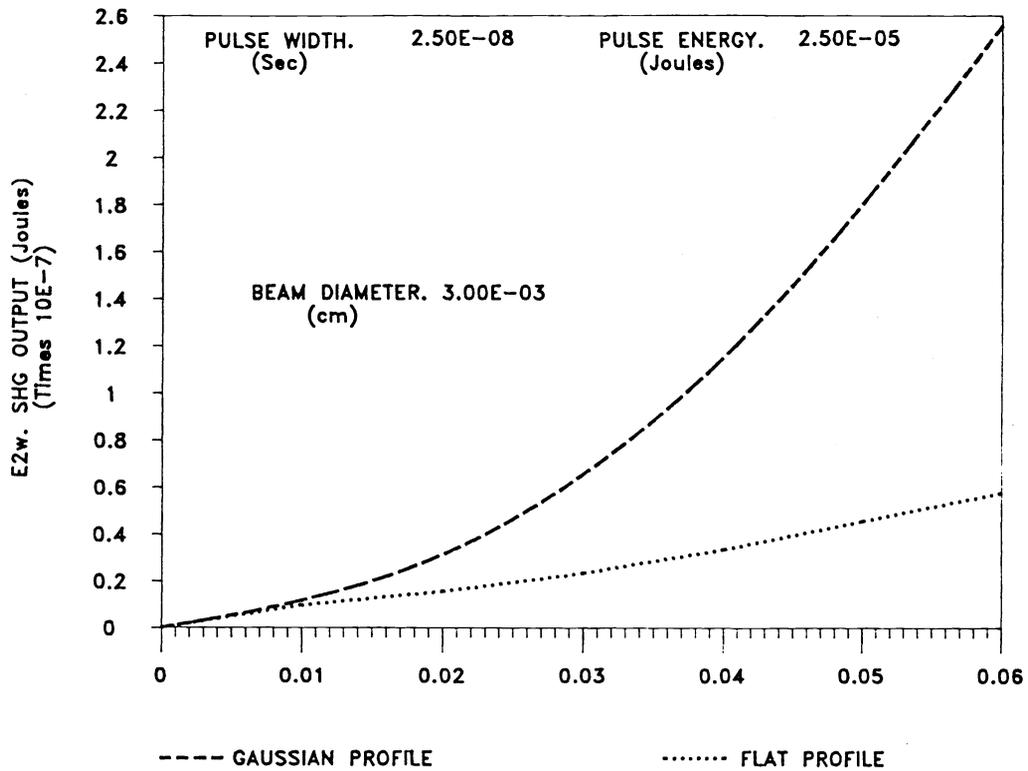

Figure 6. Harmonic output pulse energy dependence on SHG crystal length for Gaussian and Flat far field beam profiles.

Another interesting phenomenon associated with the positioning of a SHG crystal in the focal plane of a collimator is due to the quadratic intensity response of the output. It is easily shown that the square of a Gaussian function is another Gaussian of $1/\sqrt{2}$ width. Therefore, an incident fundamental beam with $1/e^2$ diameter d and Gaussian profile in the focal plane will produce an harmonic output beam of $1/e^2$ diameter $d/\sqrt{2}$. In fact, the output beam diameter may be continuously varied by defocussing, i.e. shifting the crystal along the optical axis of the collimator until the desired spot size is achieved. This will of course reduce the output pulse energy by reducing the input energy density.

Both these effects are demonstrated in Figure 7, which displays the visible emission $1/e^2$ diameter and peak intensity as measured at different positions along the optical axis of the boresight collimator. The data were obtained by placing a $25\mu m$ slit in front of the silicon detector which was translated in the image plane of the paraboloid mirror. Note that for a fundamental beam focussed on the crystal front surface (zero position) the spot diameter is indeed smaller than the laser beam spot size (~0.8d instead of 0.707d). The asymmetry in the peak intensity dependence on focal point is due to enhanced conversion efficiency as the focal plane moves into the crystal (negative values of position).
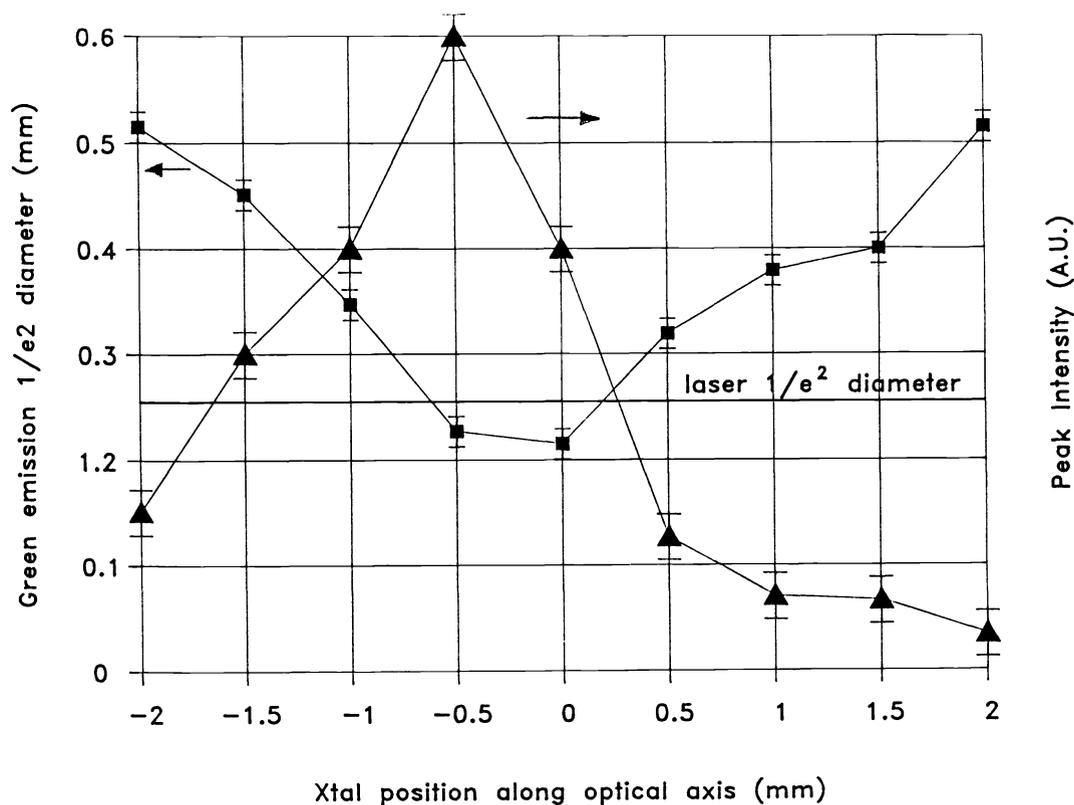

Figure 7. Peak intensity and $1/e^2$ diameter of harmonic output pulse versus crystal position along optical axis. Front surface of crystal coincides with collimator focal plane at zero position.

4. CONCLUSION

By comparing a second harmonic generating crystal with two alternative techniques (i.e. Blackbody emission and laser induced fluorescence) its superiority is demonstrated when acting as a visual target in the focal plane of a boresight collimator. Its main advantage is in conversion efficiency from $1.06\mu m$ wavelength to the visible, primarily due to the collimated reemission at $0.53\mu m$ as opposed to the lambertian nature of reemission for the alternative techniques. Furthermore, the selected crystal displays a damage threshold with the largest safety margin above the laser pulse energy to produce the required visible reemission level. The maximum boresight error expected from a KTP crystal may be calculated and is shown to be negligibly small. The spot size and visible pulse intensity may be controlled by varying crystal geometry, position along optical axis and application of anti-reflection coatings.

In summary, by correctly taking into account all of the above factors, a visual target based on a SHG crystal maintains considerable versatility, even when constraints are put on the system by other design considerations.

5. ACKNOWLEDGEMENTS

6. REFERENCES

1. Godfrey, T.E. and Clark, M.C., "Boresighting of airborne laser designator systems," Optical Engineering, Vol. 20, No. 6, p. 854, 1981.

2. Yariv, A., Optical Electronics, 3rd Ed., CBS College Publishing, p. 238-252, 1985.

3. Buhks, E., Sunstone Inc., private communication, 1989.

4. Lin, J.T. and Chen, C., "Choosing a nonlinear crystal," Lasers and Optronics, Vol. 6, p. 59, November, 1987.

5. Adhav, R.S., Adhav, S.R. and Pelaprat, J.M., "BBO's nonlinear optical phase-matching properties," Laser Focus, September 1987.

6. Stolzenberger, R.A., "Nonlinear optical properties of flux growth $KTiOPO_4$," Applied Optics, Vol. 27, No. 18, p. 3883, 1988.

7. Stolzenberger, R.A., North American Philips Corporation, private communication, 1989.